Hindawi
Advances in Civil Engineering
Volume 2018, Article ID 3210420, 10 pages
https://doi.org/10.1155/2018/3210420

Research Article

Safety Mining Technology of Coal Seams in Weathered Zone Based on Ground J-Type Pregrouting Reinforcement

Min Tu,[1] Jinlong Cai,[1,2] Hualei Zhang,[1] and Chuanxin Rong[1]

[1]*Provincial Co-Construction, Key Laboratory of Ministry of Education for High-Efficiency Safety Mining of Coal Mines, Anhui University of Science and Technology, Huainan, Anhui 232001, China*
[2]*School of Architecture and Civil Engineering, West Anhui University, Luan, Anhui 237012, China*

Correspondence should be addressed to Jinlong Cai; 25072103@qq.com

Received 17 September 2018; Accepted 18 November 2018; Published 20 December 2018

Guest Editor: Zhanguo Ma

A thin basement coal seam mining model under different overlying strata conditions was developed using the discrete element software UDEC. This approach is used to discuss the safety mining of the thin basement coal seams. Fracture development in overlying and rock strata movement law in the stope was discussed. The relationship between support and surrounding rocks under different overlying strata conditions was analyzed. Lastly, a field industrial test was conducted based on the research results. A few major conclusions could be drawn. Under load transmission in loose water-bearing strata, causing a large-scaled rock strata movement to advance into the working face is easy when only one bearing stratum exists in the overlying strata. Meanwhile, the support bears strong loads, which can easily be collapsed. When two bearing strata exist in the overlying one, the upper bearing stratum can form a voussoir beam structure. Loads on the support decreased substantially compared with those under single bearing stratum, whilst the probability of pressing frame was reduced accordingly. A weathered zone above the stope was reinforced by ground J-type drilling pregrouting, thereby improving the physical and mechanical properties and increasing the bearing capacity of the rock strata in the grouting range and safety mining of the working face in the lower coal seams. Research results provide important references for the safety mining of thin basement coal seams under similar conditions.

1. Introduction

Given the continuous increase of upper mining limit in mines in eastern and northern China, water and sand inrush accidents induced by mining of the working face in thin basement coal seams have become increasingly prominent in recent years [1]. Chinese scholars have reported extensive studies on underwater mining and accumulated substantial practical experiences given the mining technology development. However, mining in special geological conditions, such as thick loose water-bearing stratum and thin basement, continuously face a series of problems, which attributes to hydrogeological differences in various regions, water abundance in loose stratum, and increased upper mining limit. Water and sand inrush accidents occur occasionally, thereby considerably threatening the safety production of coal mines [2–4]. Safety mining in thick loose water-bearing strata also becomes a hindrance.

A series of Chinese studies have been conducted on the safety mining of a thin basement shallow seam in thick loose water-bearing strata. It is widely acknowledged that once mining-induced fractures extend upward into confined aquifers, these fractures can serve as passageways between aquifers and workings, triggering water and sand inrush. Xu et al. [5] proposed the design method of sand-prevention coal and rock pillar for the safety of the working force in loose water-bearing strata and thin basement under hydraulic loads. Guo et al. [6] suggested to maximize thin basement coal seams by reducing the mining height. Liu and Song [7–9] recommended mining based on water drainage. Guo et al. [10] and Xu et al. [11] studied the development law of fractures in overlying strata in a thin basement stope. Tan et al. and Liu et al. [12, 13] given the height of the water-conducting fractured zone is highly related to mining conditions and the lithology of the overlying strata, and empirical formulae for height estimation were given based

on numerous in situ observations. The design of waterproof pillars, water drainage mining, and mining with filling can assure safety mining of thin basement coal seams. However, given their limitations, the design of waterproof pillars is a waste of coal resources, and water drainage destroys the groundwater environment, while mining efficiency with filling has to be increased. Hence, a new thin basement mining technique should be explored to realize high-efficiency safety mining.

A hydraulic pressing frame accident occurred on the completely mechanized coal mining face 1202(3) in a thin basement coal seam in Gubei Coal Mine. The working face 1512(3) in this coal mine has similar geological conditions with those of the working face 1202(3). The manner of protecting the safety mining of the working face 1512(3) becomes one of the problems that engineering technicians have to resolve immediately.

2. Brief Introduction to the Project

The upper and lower limit heights of coal mining in the working face 1512(3) are −391 m and −497 m, respectively. The coal bed pitch is 5°–8°. Oblique mining is adopted, which has +17.32 to +22.12 m corresponding elevation. The comprehensive column graph in drilling holes #12–13 Kz4 close to the open-off cut on the working face is shown in Figure 1. The lithology of the weathered zone is mainly manifested as mudstone and sandy mudstone, which have low compressive strength values (<10 MPa).

3. Numerical Simulation Analysis of the Influences of Stratum Structures on the Migration Characteristics of Overlying Rocks in a Stope

3.1. Establishment of the Model. The working face 1512(3) was used as an engineering background in this study. A horizontal mining model was developed for the working face owing to the small coal bed pitch and for calculation convenience. The discrete element software UDEC was applied in the simulation, while the Mohr–Coulomb model was used as well. Mining models with single and double bearing layers in the overlying strata were developed (Figure 2). The model size was length × height = 200 m × 80 m. The rock mechanical parameters and the physical parameters of each rock stratum are shown in Table 1. The models were used to simulate fracture development and movement laws in the overlying strata after mining of the working face. Moreover, the models adopted fixed left, right, and lower boundaries but not free upper boundary. The measured hydraulic pressure and buried depth in a loose water-bearing layer indicated that a 11.5 MPa vertical load was applied on the upper boundary to simulate load transmission in the loose strata.

3.2. Analysis of Numerical Simulation Results. The fracture development in the overlying and rock strata movement laws when single and double bearing layers exist in the working face is shown in Figures 3 and 4, respectively.

The fracture in the rock strata above the main roof further developed as a response to the first periodic fracture of the main roof (bearing layer) when the advancing distance in the working face was 40 m (see Figure 3). When the advancing distance was 50 m, the fractures above the main roof run through a hydraulic load transmission in the loose overlying strata. This condition resulted in a large-scale subsidence of rock strata above the main roof. Under this circumstance, causing crushed hydraulic support in the working face is easy [14]. Subsequently, the rock strata above the main roof broke down with the main roof.

Fractures began to develop in the overlying rocks above the main roof (low bearing strata) when the advancing distance was 45 m (see Figure 4). When the advancing distance was 50 m, the rock strata controlled by the main roof began to sink substantially because of the periodic fracture and rotary subsidence of the main roof. The rock strata below the high bearing strata developed transverse delamination fractures, while the high bearing strata did not subside with the rotary sinking of the lower main roof. This condition was considerably different from the movement characteristic of the overlying rocks under single bearing strata. Under this circumstance, the hydraulic support only has to assume fractured rock strata from the position above the support to the positive below the high bearing strata. Subsequently, the transverse crack range expanded with the periodic fracture of the main roof, while the high bearing strata began to bend with an increase in internal cracks. When the advancing distance was 90 m, the high bearing strata began to fracture and subside, thereby forming the "voussoir beam" structure. When the pressure transmits from the overlying strata to the distant working face, the stress on the hydraulic support on the working face declined, thereby decreasing the probability of pressing frame [15].

In summary, stress on the hydraulic support decreased substantially when at least two bearing strata exist in the overlying strata in thin basement coal seams. Similarly, the probability of pressing frame was decreased. Hence, causing crushed hydraulic support on the working face when only one bearing stratum exists in the overlying strata is easy. The preceding research conclusions and previous engineering experiences indicated that a thin basement coal seam mining test should be performed by creating a high bearing stratum in the weathered zone through artificial pregrouting.

4. Grouting Reinforcement and Effect Evaluation

4.1. Grouting Scheme. A distribution pattern of J-type horizontal grouting holes on winds was designed in the weathered zone on the roof of the working face 1512 (3) in the Naner Mining Area of Gubei Coal Mine. Ground pregrouting was performed on the weathered zone at the working face roof by combining oriented drilling and horizontal pregrouting technologies. After the preset depth was reached by drilling, horizontal drilling was initiated, while the vertical profile was in J-shape. The horizontal drilling holes were in wing-shaped distribution. This distribution of pregrouting holes was novel and applicable to

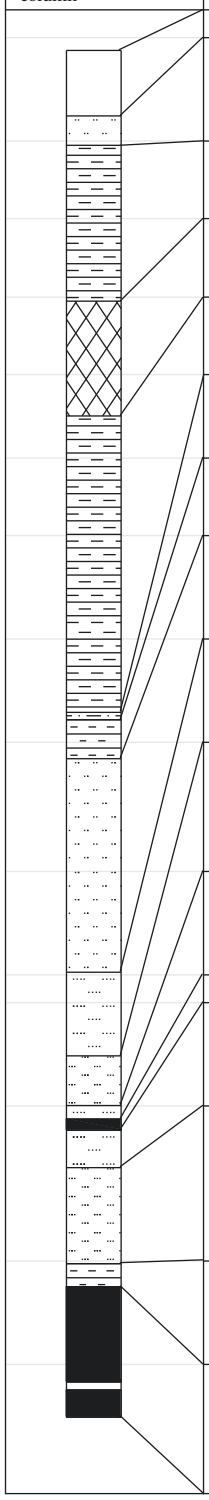

Lithological geological column	Rock type	Strata thickness (m)	Tithological description
	Gravel clay	2.9	
	Weathered medium sandstone	1.3	Shallow khaki, medium grain structure, muddy cementation, rock composition mainly composed of quartz feldspar, less dark minerals, denser, harder, weathering degree.
	Weathered mudstone	6.9	Mottled, khaki mixed reddish brown, green, muddy structure, horizontal bedding, weathering phenomenon is strong, brittle.
	Weathered mottled mudstones	5.08	Mainly gray, with purple, gray and rust yellow, mainly muddy, with aluminum soil, massive structure.
	Weathered mudstone	13.12	Mottled, khaki mixed reddish brown, green, muddy structure, horizontal bedding, weathering phenomenon is strong, brittle.
	Weathered carbonaceous mudstone	0.33	
	Weathered mudstone	1.72	Mottled, khaki mixed reddish brown, green, muddy structure, horizontal bedding, weathering phenomenon is strong, brittle.
	Weathered medium sandstone	9.45	Shallow khaki, medium grain structure, muddy cementation, rock composition mainly composed of quartz feldspar, less dark minerals, denser, harder, weathering degree.
	Siltstone	3.7	Gray, local weathering is earthy yellow, uniform structure, visible muscovite shavings, containing carbon particles. With horizontal bedding, plant fossil debris can be seen.
	Fine sandstone	2.2	Blue-gray, quartz-feldsparis the main, subbrown, granules <distributed in belts> uniform structure, occasionally volcanic inclusions with good roundness, mud-iron cementation, intermittent intermittent wave-like bedding.
	Siltstone	0.61	Gray, local weathering is earthy yellow, uniform structure, visible muscovite shavings, containing carbon particles. With horizontal bedding, plant fossil debris can be seen.
	Coal	0.48	Black, soft, fragile, partially missing.
	Siltstone	1.66	Gray, local weathering is earthy yellow, uniform structure, visible muscovite shavings, containing carbon particles. With horizontal bedding, plant fossil debris can be seen.
	Fine sandstone	4.25	Blue-gray, quartz-feldsparis the main, sub-brown, granules <distributed in belts> uniform structure, occasionally volcanic inclusions with good roundness, mud-iron cementation, intermittent intermittent wave-like bedding. Local phase changes to sandy mudstone.
	Mudstone	1.03	Dark gray, sand-grain structure, blocky, brittle, there are many cracks and slip surfaces, top with rhomboid, occasionally mixed with thin strips of carbonaceous mudstone.
	13-1 coal	4.2 (0.37) 1.19	Black, upper block, powdery, a small amount of scaly, oily luster, bright coal, dark coal, dark scaly, a small block, with glass luster, semidurain~semiclarain, often mixed with a thin layer of sandwich.

Figure 1: Drilling histogram.

pregrouting reinforcement in the weathered zone at the working face roof.

4.2. Grouting Parameters. The grouting adsorption capacity of the surrounding rocks was considerably different owing to various lithologies, fracture development degrees, and loose ranges. Moreover, such capacity was influenced by grouting pressure and time. In principle, grouting will be continued until the termination of the grouting adsorption to assure compact filling in fractures.

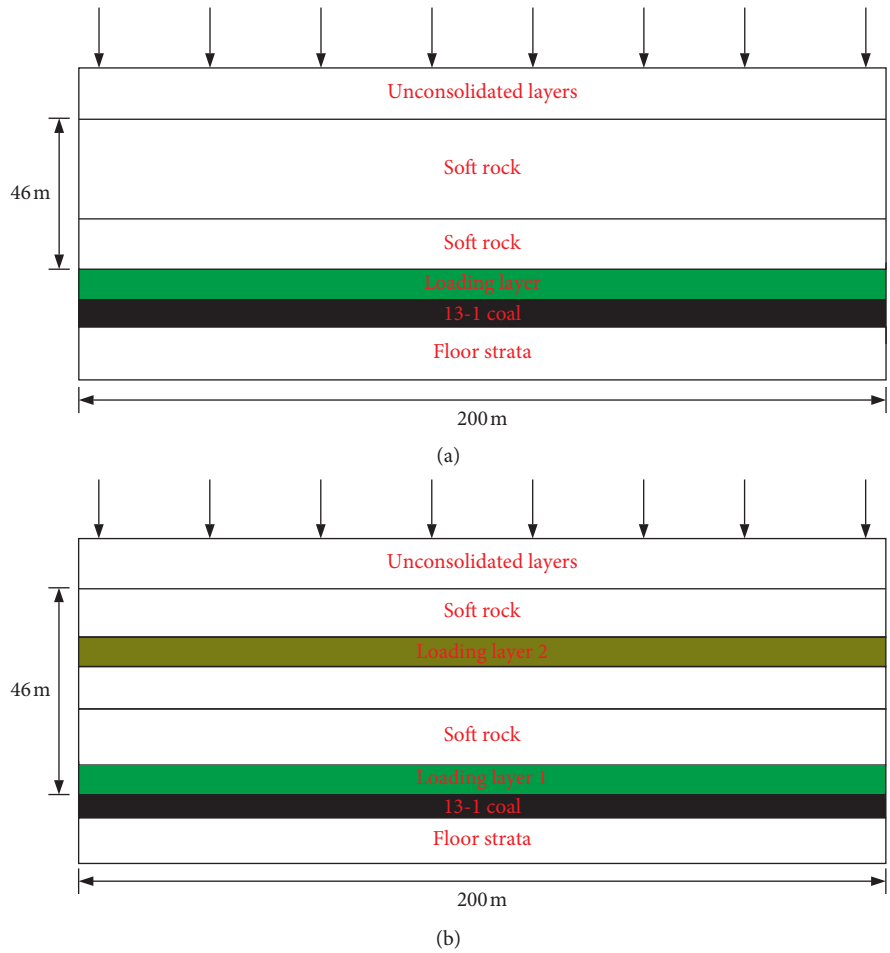

Figure 2: Numerical calculation model diagram: (a) single bearing stratum and (b) double bearing strata.

Table 1: Mechanical properties of coal and rock.

Lithology	Cohesive force (MPa)	Internal friction angle (°)	Uniaxial compressive strength (MPa)	Elastic modulus (GPa)	Poisson's ratio	Tensile strength (MPa)
Unconsolidated layers	12.89	34.70	92.10	25.35	0.20	15.54
Loading layer 2	3.16	41.30	34.51	9.87	0.25	4.93
Soft rock	4.50	38.5	30.5	10.56	0.28	3.82
Loading layer 1	5.36	42.50	35.28	11.45	0.24	5.19
13# coal	0.48	28.6	7.65	2.96	0.30	0.86
Floor strata	7.69	40.60	45.68	15.36	0.23	7.85

(1) A pore diameter in the grouting section was designed φ152 mm.

(2) Follow-up grouting: grouting was performed every 30 m and advances continuously thereafter.

(3) The diffusion radius of grouting was 15 m.

(4) Grouting range: 60 m long along the stride of the working face and 200 m wide along the inclined direction.

(5) Grouting volume: 386, 460 m^3.

(6) The single liquid was adopted and the rock fracture rate was 8%.

(7) The grouting amount was calculated as follows:

$$Q = \frac{\lambda V \eta \beta}{n}, \tag{1}$$

where λ is the loss coefficient of the grouting liquid ($\lambda = 1.1$), V is the grouting volume ($V = 386, 460\ m^3$), H is the fracture rate ($\eta = 9\%$), B is the filling rate of the grouting liquid ($\beta = 0.8$), and n is the setting percentage of the grouting liquid (0.9). Therefore, $Q = 1.1 \times 386, 460 \times 8\% \times 0.8/0.9 = 30{,}230\ m^3$.

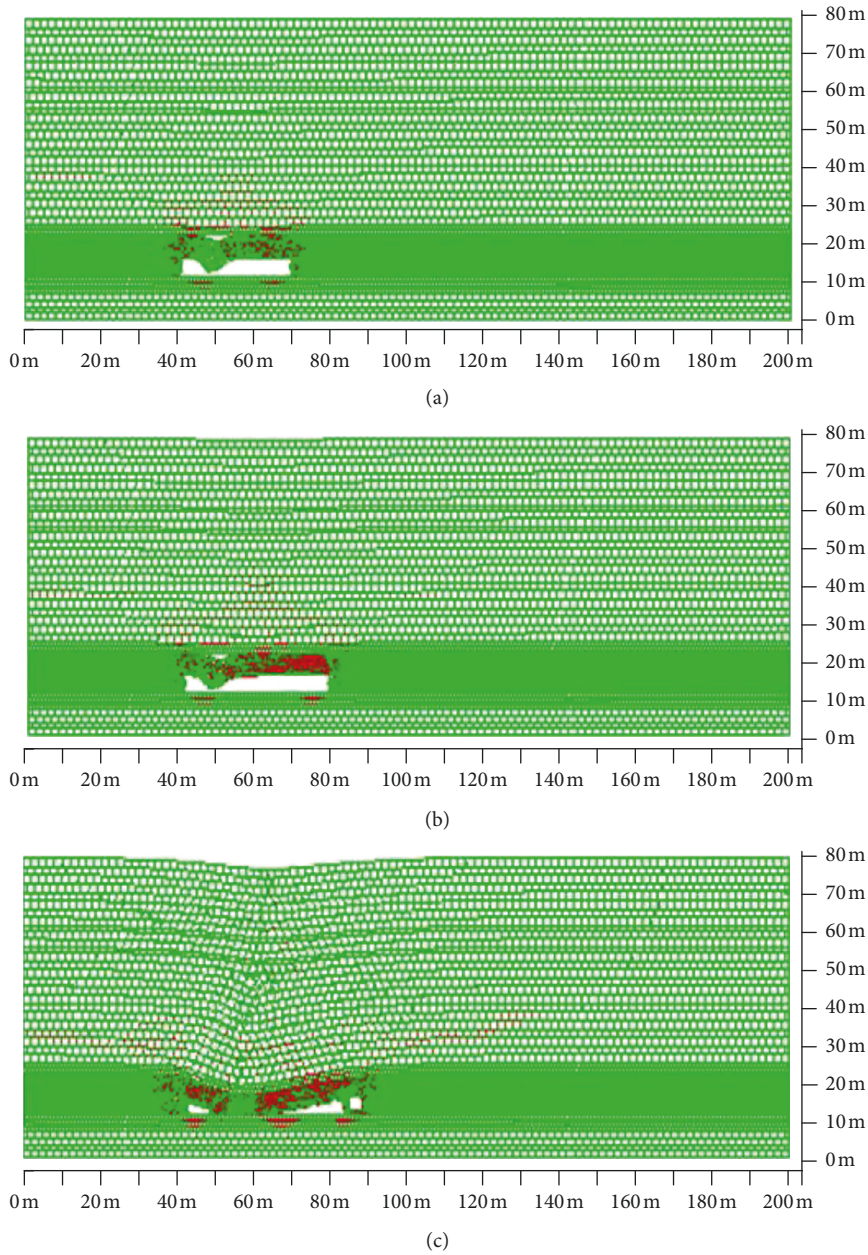

Figure 3: Movement law of the overburden strata when only one hard rock exists: advancing distances of the working face are (a) 30 m, (b) 40 m, and (c) 50 m.

The grouting material used P.O42.5 ordinary Portland cement. The single-liquid ordinary Portland cement slurry was prepared, while the water-cement ratio ranged between 0.6 : 1 and 0.75 : 1. The single liquid occupied the dominant role.

The cement content was approximately $T = 35{,}200 \times 0.75 = 22{,}673$ (tons).

Four grouting holes were designed. The distances of the #1 to the #2 and 3# holes were 30 m and 40 m, respectively. The distribution profile of the grouting holes is shown in Figure 5.

The grouting depth in the weathered mudstone strata was designed to be 434.43–447.55 m. The grouting length from the airway 1512(3) to the region above the machine land 151(3) was designed to be 200 m. The grouting width from the open-off cut of the working face to the region 60 m above the stope direction was designed to be 60 m.

The theoretical and numerical calculations indicated that the grouting pressure was set to be 10 MPa initially. The grouting material with the P.O42.5 ordinary Portland cement and single-liquid ordinary Portland cement slurry was prepared. The water-cement ratio was 0.6 : 1–0.75 : 1, while the single liquid was the dominant material.

4.3. Grouting Effect. The comprehensive column graphs of the #13–#13 Kz4 holes in Figure 1 show that the region in

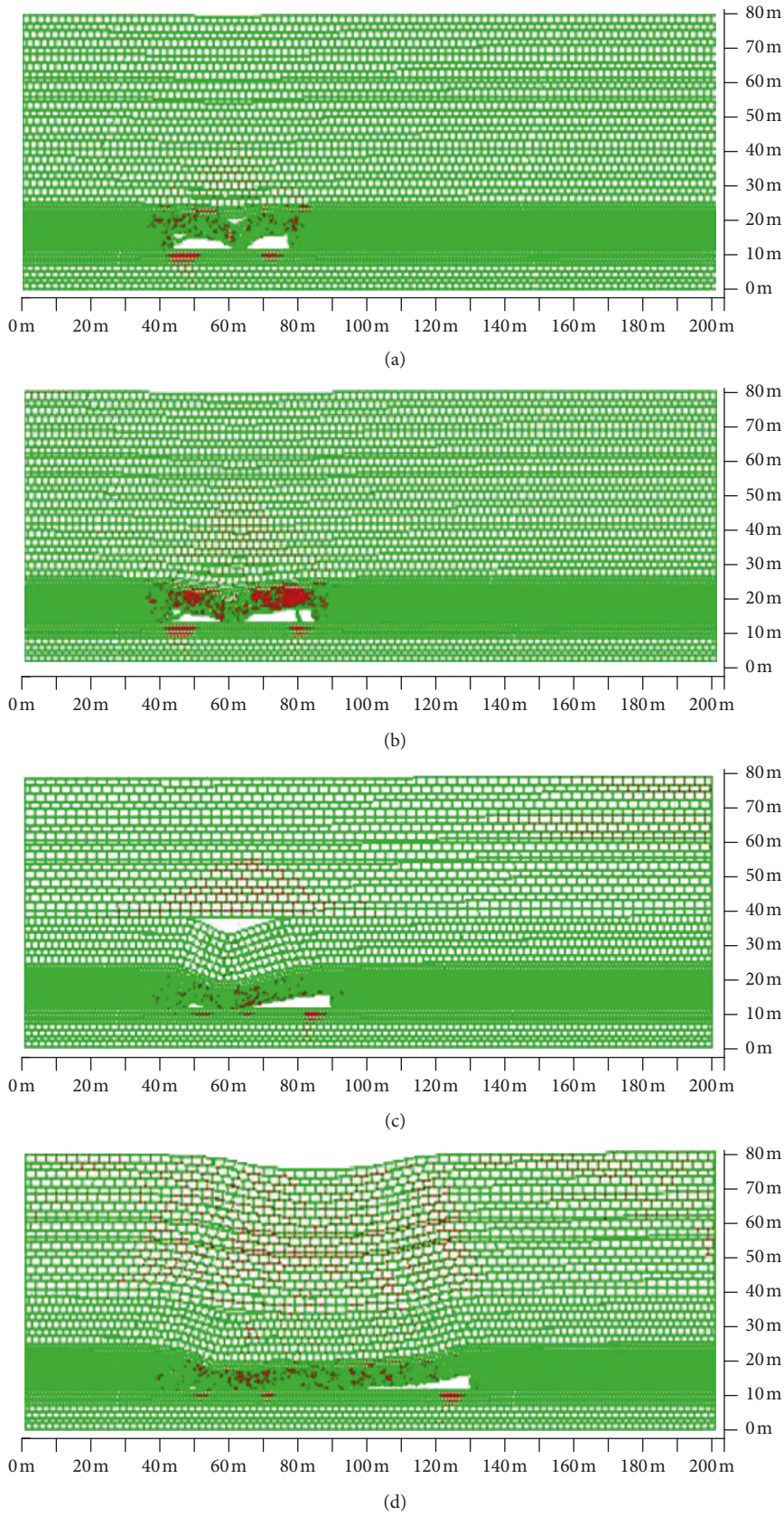

Figure 4: Movement law of the overburden strata when two hard rocks exist: advancing distances of the working face are (a) 35 m, (b) 45 m, (c) 50 m, and (d) 90 m.

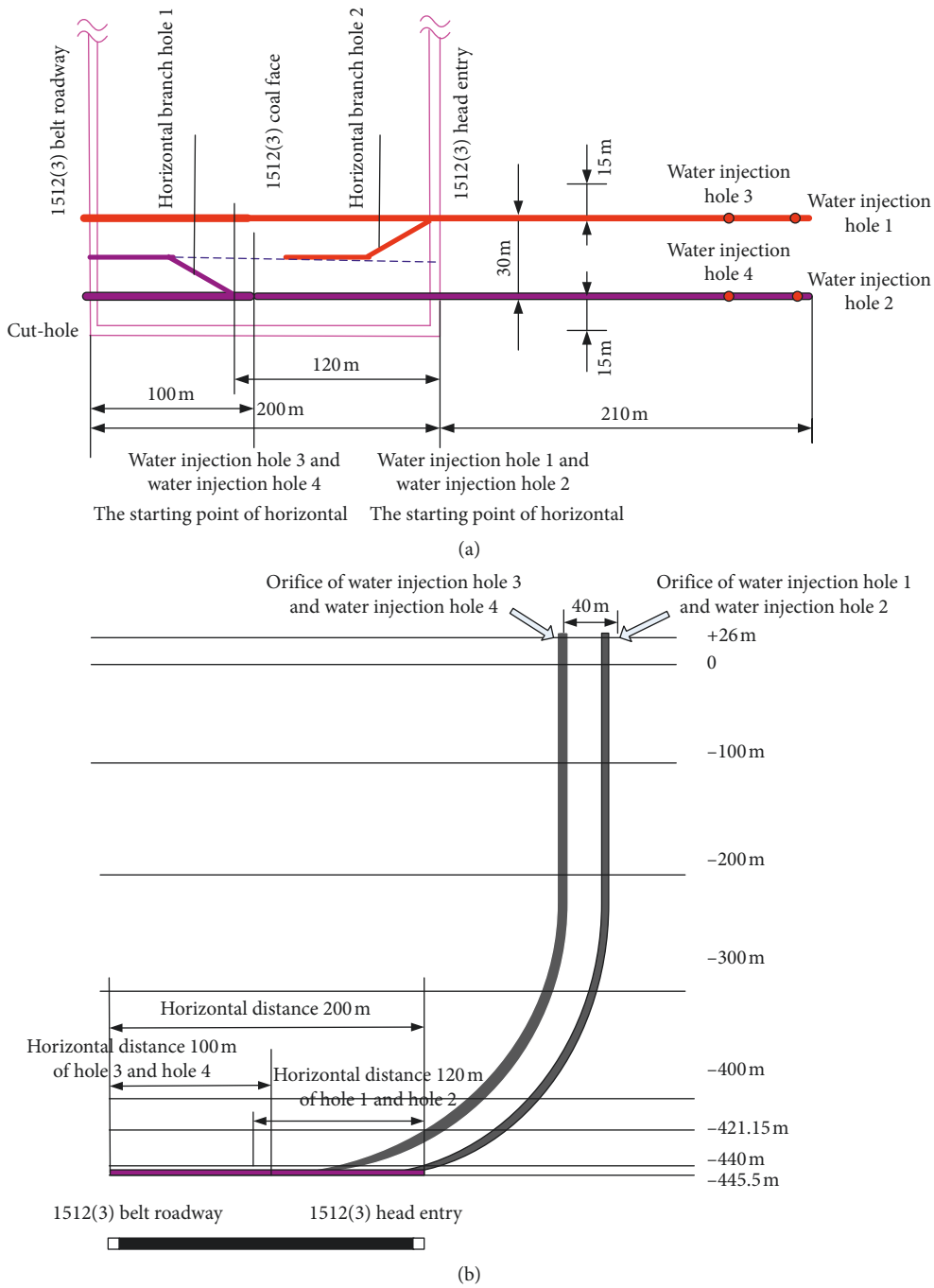

Figure 5: Ground J-type grouting hole distribution: (a) plan and (b) profile views.

20–50 m above the coal seam roof was the weathered zone. The characteristics of the grouting diffusion indicated that this grouting was implemented in the 434.43–447.55 m deep weathered mudstone layer.

Rocks before and after the grouting were observed through SEM. Rock cores in the same layer in the grouting and nongrouting sections were selected in preparation of the scanning samples to observe the microscopic changes of rocks before and after grouting (Figure 6). In the weathered zone without grouting reinforcement, rock mass showed a rough surface and an evident defect. Rock mass was relatively smooth in the weathered zone with grouting reinforcement. High-pressure grouting relatively compacts and fills the microscopic defects in the weathered rock mass. The mudstone core in the weathered zone was crushed, while the nonrock core conformed to the experimental standards. A shearing resistance experiment was conducted with a few nonstandard specimens with approximately 16.5–45 mm height. The experimental results reflected that the mean values of the shear strength and cohesion were increased by approximately 40%. Grouting can substantially improve the strength of the mudstone in the weathered zone.

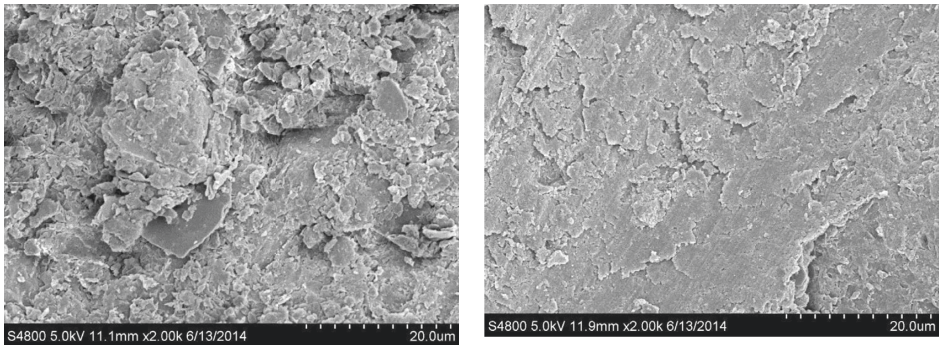

(a) (b)

Figure 6: Comparison of the microstructures of rock masses in the weathered zone (2000 magnifications, 20 $\mu\varepsilon$): microstructure of the samples in the (a) unreinforced section and (b) after grouting reinforcement.

5. Stress Analysis on Supports before and after Grouting

The relation curve between the support and the surrounding rocks was drawn based on the numerical calculation results and reference [16] to compare the stresses on the hydraulic supports before and after the grouting (Figure 7).

When two key layers exist in a thin basement below the loose water-bearing strata, the calculation formula of the working resistance (P_1) of support in Figure 7(a) is as follows [17]:

$$P_1 = (Q_1 + \xi Q_2)\cos\alpha \cdot K, \tag{2}$$

where Q_1 is the weight of rock mass ① from the region above the support to the direct roof below key layer 1 (kN/m^3) and ξQ_2 is the force applied by the rotation of knife-shaped rock mass ② below the key layer 2 on rock mass ① (kN/m^3).

The calculation formula of working resistance of support in Figure 7(b) is as follows:

$$P_2 = [Q_1 + \xi Q_2' + \mu Q]\cos\alpha \cdot K, \tag{3}$$

where Q_1 is the weight of rock mass ① from the region above the support to the direct roof below key layer 1 (kN/m^3), ξQ_2 is the force applied by the rotation of the knife-shaped rock mass ② below the key layer 2 on rock mass ① (kN/m^3), and μQ is the force applied by the effect from the loose water-bearing strata on the roof of rock mass ②.

Figure 7 shows that the range of rock mass ② above the single bearing stratum in Figure 7(b) was substantially larger than that above the two bearing strata in Figure 7(a). Hence, ξQ_2 is substantially smaller than ξQ_2. Moreover, P_2 involves the additional pressure from the loose water-bearing strata μQ compared with P_1. Accordingly, the working resistance of support when two bearing strata exist in a thin basement is considerably lower than that under single bearing stratum.

6. Roof Stability and Strata Behavior Characteristic

Real-time monitoring of the working resistance of support in the working face was conducted to the protect safety mining of the working face. The three-dimensional contour map of the working resistance of the hydraulic support was drawn based on the monitoring results (Figure 8).

When the advancing distance was 70 m (i.e., the third period pressure on the working face), the working resistance of the hydraulic support was substantially higher than those of the previous two periods (see Figure 8). Accordingly, this hydraulic stress is a large period pressure. At this moment, the working face experienced three small periodical weightings. When the advancing distance is 120 m, the working face developed the second strong periodical weighting (see Figure 8). At this point, the working face experienced seven periodical weightings, thereby conforming to previous numerical simulation results.

The step distance of periodical weighting during the initial period at different positions of the working face was 13–15 m. With regard to the advances to the working face, the step distance of periodical weightings at different positions of the working face began to decrease to 11–13 m after the 8th periodical weighting. The initial weighting step distance on the basic roof at different positions of the working face was 27.7–36.5 m, with an average of 31.5 m. The periodical weighting step distance on the basic roof at different positions of the working face was 9.9–18.3 m, with an average of 13.20 m. In particular, the weighting step distance in the middle range of the stope was small, but the step distances at the upper and lower ends were relatively large. The initial and periodical weighting step distances were slightly higher than those on the working face without grouting reinforcement under similar conditions.

7. Conclusions

In this study, the working face 1512(3) in a thin basement coal seam in Gubei Coal Mine is used as the research object. The roof stability of different strata structures on this working face is discussed through numerical analysis, laboratory test, and field investigation. The following major conclusions are drawn:

(1) Under the load transmission in loose water-bearing strata, causing a large-scaled roof subsidence in the overlying strata when a single bearing stratum exists

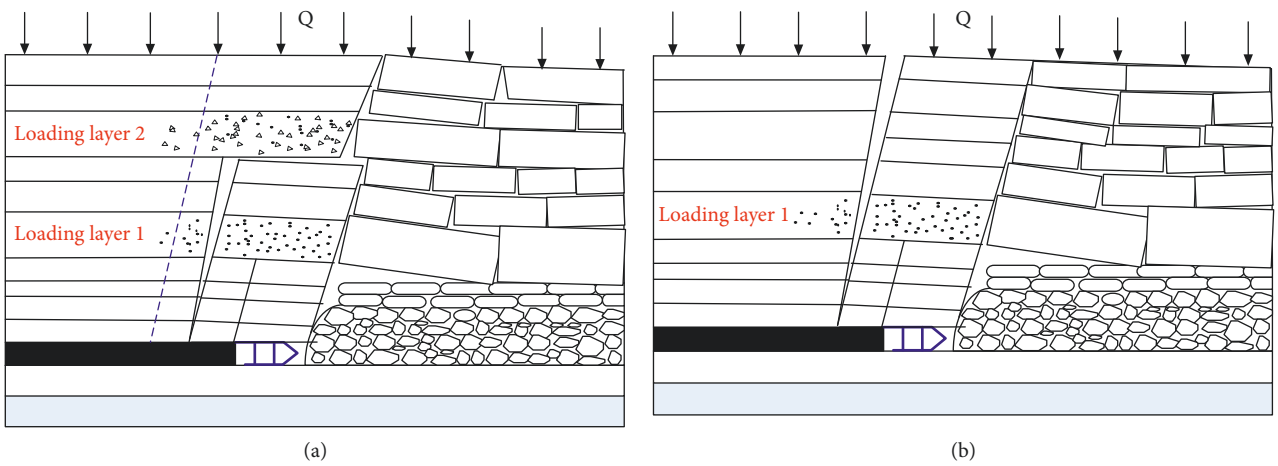

Figure 7: Working face hydraulic support that surround the rock relations: (a) double and (b) single bearing layer structures.

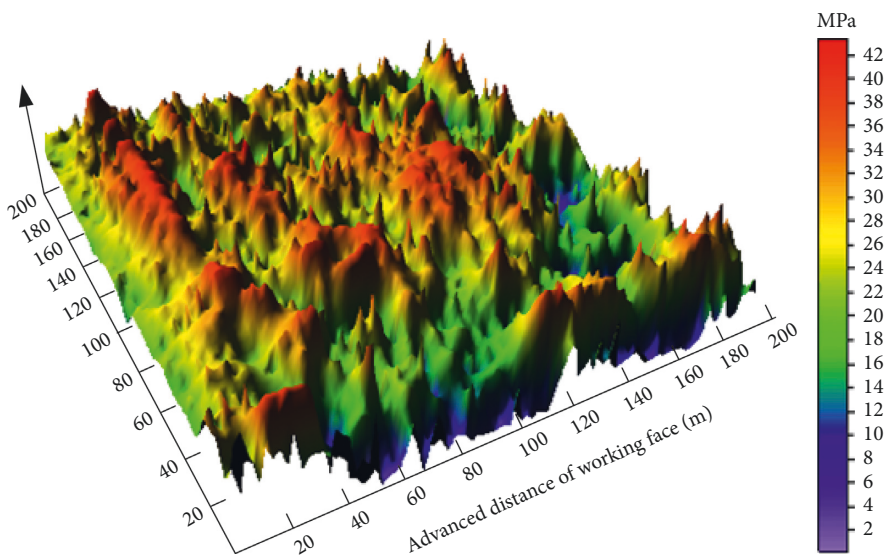

Figure 8: Face hydraulic support working resistance contour map.

is easy, thereby inducing pressing frame accident. When two bearing strata exist, the upper one can transmit pressure from the overlying strata to the distancing position away from the working face. The probability of pressing frame is decreased.

(2) After ground grouting in the weathered zone, the mean values of the shear strength and cohesion of the mudstone in the weathered zone are increased by approximately 40%. This result indicates that grouting can substantially improve the mudstone strength in the weathered zone.

(3) The overall reinforcement of the weathered zone is conducive to realize the safety mining of the working face. "Large and small periodical" weighting phenomena in recovery are observed. Moreover, the initial and periodic weighting step distances are higher than those on the working face without grouting reinforcement under similar conditions. The slurry achieves the expected reinforcement effect.

Data Availability

The data supporting the conclusions of the study can be accessed from this research article. The nature of the data used in the study is the laboratory experimental data, the field observation data, and the theoretical calculation data. The laboratory experimental data used to support the findings of this study are included within the article; mainly the mechanical parameters used to support the findings of this study are available from the corresponding author upon request. The field observation data used to support the findings of this study are included within the article; the grouting parameters are shown in Section 4.2 and the grouting hole setting is shown in Figure 5. The theoretical calculation data used to support the findings of this study are available from the corresponding author upon request.

Conflicts of Interest

The authors declare that they have no conflicts of interest.

Authors' Contributions

All authors contributed to the publication of this study. Min Tu conceived and designed the experiments, revised and reviewed the manuscript, and wrote the corresponding paper; Jinlong Cai performed the experiments; and Hualei Zhang analyzed the data.

Acknowledgments

This study is part of the projects financially supported by the Chinese National Natural Science Foundation (NSFC; Grant nos. 51574007 and 51604007). The authors gratefully acknowledge the financial support received from NSFC.

References

[1] X. J. Wang, *Study on occurrence condition and prevention of support crushing and water inrush disaster during mining and unconsolidated confined aquifer*, Ph.D. thesis, China University of Mining and Technology, Xuzhou, China, 2014, in Chinese.

[2] X. H. Xu and J. Wang, *Study on Forecast and Forecast of Coal Mine Water Inrush*, The Geological Publishing House, Beijing, China, 1992, in Chinese.

[3] W. H. Sui, Y. K. Liang, and G. L. Zhang, "Study status and outlook of risk evaluation on water inrush and sand inrush mechanism of excavation and mining," *Journal of Coal Science & Technology*, vol. 39, no. 11, pp. 5–9, 2011, in Chinese.

[4] G. Q. Xu, Y. B. Hu, and M. Tu, "Review and discussion on rational height of safety coal and rock pillars under soft water bearing strata," *Journal of Coal Science & Technology*, vol. 31, pp. 41–44, 2003.

[5] Y. H. Xu, M. Z. Du, and J. H. Li, "Instability mechanism and design method of coal and rock pillar under water pressure," *Journal of China Coal Society*, vol. 42, no. 2, pp. 328–334, 2017, in Chinese.

[6] Z. P. Guo, Z. J. Wen, and F. Q. Wang, "Study on improving upper limit in thick seams slicing mining under thick alluvium," *Journal of China Coal Society*, vol. 33, no. 11, pp. 1220–1223, 2008.

[7] J. Liu, "Feasibility study of dewatering and depressurizing of high pressure roof water," *Journal of China Coal Engineering*, vol. 48, pp. 42–45, 2016.

[8] Y. J. Song, "Method to determine pre-drainage and safety water level in aquifer of roof before mining operation," *International Journal of Coal Science & Technology*, vol. 45, pp. 161–165, 2017.

[9] J. J. Chen, W. P. Guo, and Y. F. Zou, "Feasibility study on safety under large scale water bodies," *Chinese Journal of China Safety Science Journal*, vol. 21, pp. 57–62, 2011, in Chinese.

[10] W. B. Guo, D. M. Yang, and Y. Tian, "Study on safety of overlying strata by backfilling in water-preserved mining under thick alluvium and thin bedrock," *International Journal of Mining Science and Technology*, vol. 31, pp. 220–225, 2014.

[11] P. Xu, Y. J. Zhou, and M. X. Zhang, "Fracture development of overlying strata by backfill mining under thick alluvium and thin bedrock," *International Journal of Mining Science and Technology*, vol. 32, pp. 617–622, 2015.

[12] Y. L. Tan, X. S. Liu, J. G. Ning, and Y. W. Lu, "In situ investigations on failure evolution of overlying strata induced by mining multiple coal seams," *Geotechnical Testing Journal*, vol. 40, no. 2, article 20160090, 2017.

[13] State Bureau of Coal Industry, *Pillar Design and Mining Regulations under Buildings, Water, Rails and Major Roadways*, China Coal Industry Publishing House, Beijing, China, 2000, in Chinese.

[14] J. L. Xu, X. Z. Wang, and W. T. Liu, "Effect of primary key stratum location on height of water flowing fracture zone," *Chinese Journal of Rock Mechanics and Engineering*, vol. 28, pp. 380–385, 2009.

[15] X. Z. Wang, J. L. Xu, and W. B. Zhu, "Overburden structure influence to support crushing and water inrush during mining under unconsolidated confined aquifer," *Journal of Mining & Safety Engineering*, vol. 31, pp. 838–844, 2014, in Chinese.

[16] H. L. Zhang, M. Tu, and H. Cheng, "Roof leakage mechanism and control technology study of fully mechanized large mining height mining face of thin bedrock seams," *Chinese Journal of Rock Mechanics and Engineering*, vol. 38, pp. 1697–1704, 2018, in Chinese.

[17] Z. H. Li, X. Z. Hua, and K. Yang, "Relation between support and supporting rocks and its influence on strata behaviors in working face with a raise of mining upper limit," *Chinese Journal of Rock Mechanics and Engineering*, vol. 34, pp. 1162–1171, 2015.